Stabilized Polymer Microparticles by Precipitation with a Compressed Fluid Antisolvent. 1. Poly(fluoro acrylates)

Simon Mawson,[†,‡] Keith P. Johnston,*[,†] Doug E. Betts,[§] Jim B. McClain,[§] and Joseph M. DeSimone[§]

Department of Chemical Engineering, University of Texas, Austin, Texas 78712-1062, and Department of Chemistry, University of North Carolina, Chapel Hill, North Carolina 27599-3290

Received July 16, 1996; Revised Manuscript Received November 4, 1996[⊗]

ABSTRACT: Poly(1,1-dihydroperfluorooctyl acrylate) (poly(FOA)) based stabilizers greatly reduce, and in some cases eliminate, flocculation of amorphous poly(methyl methacrylate) (PMMA) and polystyrene (PS) microparticles formed by precipitation into liquid CO_2 at 23 °C. The microparticle stabilization mechanism is explained in terms of the stabilizer−CO_2 phase behavior, the spray characteristics, and the interfacial activity of the stabilizer. Compared with the homopolymer poly(FOA), the diblock copolymer PS-*b*-poly(FOA) produces smaller and more spherical primary particles (0.1−0.3 μm) and also prevents flocculation at lower stabilizer concentrations. These differences are due to the greater interfacial activity of PS-*b*-poly(FOA). Steric stabilization commences in the jet on the order of several tenths of milliseconds and continues for seconds throughout the precipitator. With the use of a coaxial nozzle, precipitation is delayed and the stabilizers become even more effective at preventing flocculation.

Introduction

In 1992, Dixon[1] demonstrated a spray process for forming a wide variety of polymeric microstructures by precipitation with a compressed fluid antisolvent (PCA). In PCA, an organic solution is sprayed through an atomization nozzle into cocurrently flowing CO_2. CO_2 is an antisolvent (either as a gas, liquid, or supercritical fluid) for the solute (polymer), but is miscible with the solvent. The two-way mass transfer of solvent into CO_2 and CO_2 into the solution precipitates the polymer. The diffusion is much faster in both directions than in the case of conventional liquid antisolvents. Because of rapid phase separation, particles and fibers have been produced with submicron features. Such small features and high surface areas are uncommon with conventional liquid antisolvents. They are more typical of another high pressure process, rapid expansion of supercritical solutions (RESS),[2−8] suggesting similar characteristic times for phase separation. By changing the solution concentration, temperature, and the relative CO_2 to solution flow rate, a wide variety of morphologies have been produced, including 100 nm−8.0 μm amorphous and semicrystalline microspheres and microparticles;[1,9−12] 100 nm−1.0 μm highly oriented microfibrils of amorphous,[1,13] liquid crystalline,[14,15] and semi-crystalline polymers;[16] 0.1−1.0 μm bicontinuous networks;[1] 100−300 μm hollow and porous fibers;[1,13] 100−500 μm microballoons with porous shells;[1,17] encapsulated drug delivery systems,[18,19] and metastable polymer blends.[20]

It is difficult to produce uniform microspheres by PCA, as flocculation and agglomeration are usually present. Semicrystalline poly(L-lactic acid) (L-PLA) microspheres formed by PCA at T = 31 °C were not flocculated,[10,18] whereas amorphous polystyrene (PS) particles were highly flocculated and agglomerated.[9,12] For PS, the degree of agglomeration increases significantly with the temperature of the spray. Flocculation is even more severe for amorphous poly(methyl methacrylate) (PMMA). Exposure of PMMA particles to CO_2 at a pressure and temperature of 69 bar and 23 °C can lead to such severe agglomeration that primary particles are no longer discernible.[21] The degree of flocculation and/or agglomeration of amorphous polymers upon exposure to CO_2 is directly related to the glass transition temperature, T_g, and the viscoelastic behavior of the polymer. This plasticization of the polymer by CO_2 complicates the ability to control microstructure in the PCA process.

Recently, theoretical models[22−24] and experimental data[25−28] have been developed for the glass transition temperature and pressure, P_g, of amorphous polymers with large amounts of dissolved CO_2. Four fundamental types of T_g versus P_g behavior have been predicted with a lattice fluid model,[23] and three of these types have been confirmed experimentally.[26,27] For PS, the T_g is depressed to approximately 31 °C for a CO_2 pressure of 70 bar. In contrast, PMMA is plasticized down to 0 °C, due to the higher CO_2 solubility. The PMMA−CO_2 system exhibits retrograde vitrification, where the glassy polymer becomes a liquid upon cooling at constant pressure, due to an increase in dissolved CO_2. The T_g is depressed in proportion to the sorption of CO_2, which can be a potent plasticizer.[27]

Our goal is to minimize the problem of flocculation in the PCA process to enable the formation of uniformly sized microparticles or microspheres. This is to be accomplished by adding a polymeric stabilizer to CO_2 to sterically stabilize the precipitating polymer microstructure. The stabilizer must contain a highly "CO_2-philic" group[29] which is solvated by the CO_2 continuous phase. A key advancement was the demonstration of the ability of the amorphous fluoropolymers poly(1,1-dihydroperfluorooctyl acrylate) (poly(FOA)) and polystyrene (PS)-*b*-poly(FOA) to stabilize PMMA[29,30] and PS[31] latexes formed by dispersion polymerization in CO_2. Micrometer-sized particles with a narrow size distribution were formed with molecular weights above 100 000. On the basis of measurements of interfacial tension and emulsion stability, steric stabilization of polyacrylate emulsions by poly(FOA) is likely due to a small number of adsorbed segments and a large number of segments in loops and tails.[32]

[†] University of Texas.
[‡] Current address: Union Carbide Corp., South Charleston, WV 25303.
[§] University of North Carolina.
[⊗] Abstract published in *Advance ACS Abstracts,* December 15, 1996.

S0024-9297(96)01048-0 CCC: $14.00

The architecture of stabilizer chains anchored to latexes in supercritical fluids has been predicted theoretically.[33] A lattice fluid self-consistent field theory was developed to show that the stability of a latex is influenced by the compressibility of a supercritical fluid, which contributes to the positive entropy gain associated with removing solvent from the chains of the stabilizer near the particle surface.[33]

Few polymeric stabilizers are CO_2-philic. Examples of CO_2-philic groups include fluoroacrylates, fluoro ethers, and siloxanes.[8,34−42] Stabilizers with fluoro ether tails have been used to form reverse micelles in CO_2[34] and water-in−CO_2 microemulsions with "bulklike" water cores that can uptake proteins.[42]

Our objective is to show that a polymeric stabilizer can prevent flocculation and agglomeration of PMMA and PS in the PCA process. Here the time frame for stabilization of the suspended particles is much shorter than in dispersion polymerization.[20] Since PMMA is so highly plasticized by CO_2 and has a large tendency to flocculate and agglomerate even at room temperature, the stabilization of PMMA particles is particularly challenging. The homopolymer, poly(FOA), and the diblock copolymer, PS-*b*-poly(FOA), were selected as stabilizers, on the basis of their high solublities in CO_2[30] and the above success for forming PMMA and PS latexes by dispersion polymerization. Mixtures of the two stabilizers were used to reduce the concentration of the PS-*b*-poly(FOA). The morphology of the product is explained in terms of the stabilizer concentration in the flowing CO_2, the flocculation mechanisms, the stabilizer−CO_2 phase behavior, the spray characteristics, and the depressed glass transition temperature of the polymer. To determine the effects of turbulence and mixing, the nozzle geometry was varied to change the velocity of the flowing CO_2.[12]

There are three different types of benefits of this study. The first is the demonstration of the ability to form uniform nonflocculated particles by the PCA process. The second is a clearer understanding of the mechanism for the development of morphology in PCA, since the complication of flocculation can be minimized. The third is a new means to generate latexes of submicron particles in CO_2 and to study stabilization mechanisms.

Experimental Section

Materials and Characterization. Poly(methyl methacrylate) (PMMA) (M_w = 75 000; Scientific Polymer Products Inc.) and PS (Pressure Chemical) with a M_w of 200 000 and a M_w/M_n of 1.05 were used as received. The solvents were spectrophotometric grade methyl ethyl ketone (MEK) (Mallinkrodt) and toluene (EM Science). Poly(FOA), prepared by solution free-radical polymerization in supercritical CO_2 as described previously,[36] had a molar mass of 1.0×10^6 g/mol as determined by small angle neutron scattering.[43] The PS-*b*-P(FOA) was synthesized using an "iniferter" technique described elsewhere and had a M_n of 3.7K/27.5K.[44] Instrument grade CO_2 was used for all experiments.

The polymer morphology was analyzed and imaged with a Jeol JSM-35C scanning electron microscope (SEM). Samples were sputter coated with gold-palladium to a thickness of approximately 200 Å.

Apparatus. Figure 1 shows the experimental PCA apparatus, which is based on earlier versions.[1,16] The stabilizer/CO_2 solution was prepared in a 1.75 cm i.d., 42 mL stainless steel tube containing a piston with two Buna-N O-rings and agitated with a stir bar. The composition of this solution was constant during the spray process.[30] The polymer solution was added to a high pressure automated syringe pump (ISCO Inc., model 100D) and sprayed into a 1.27 cm i.d., 13 mL sapphire tube containing the flowing CO_2/stabilizer solution. The precipitation was observed visually.[1,12,16]

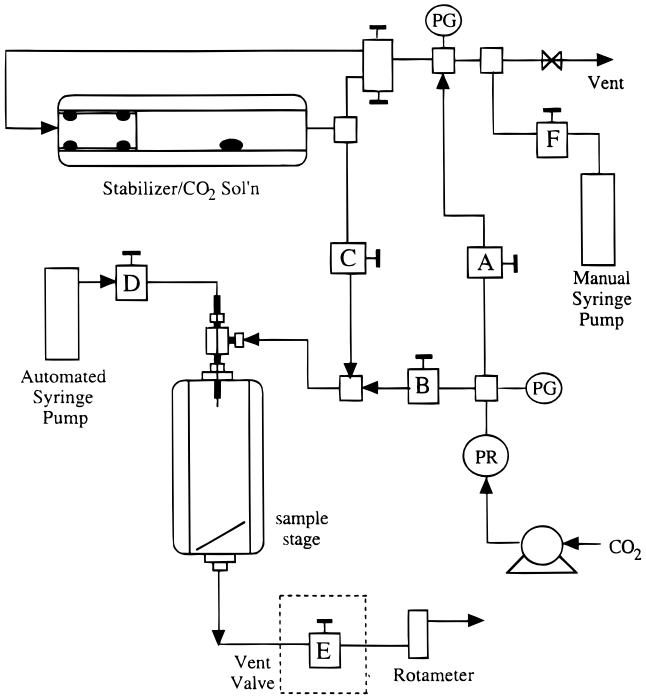

Figure 1. Schematic of the variable volume view cell and sapphire precipitator apparatus used for PCA with fluoro acrylate stabilizers (PR, pressure regulator; PG, pressure gauge).

A 50 μm i.d. × 16.5 cm long fused silica capillary tube (Polymicro Technology) was used to atomize the solution. The capillary tips were inspected with a microscope to ensure that the ends were smooth. Two types of nozzles were used. In the standard nozzle, the CO_2 phase was introduced at low velocity (0.5 cm/s) well above the capillary, whereas it was introduced at high velocity (165 cm/s) in an annular region about the capillary tube in the coaxial nozzle.[12] The inside and outside diameters of the annular region were 0.030 in. (760 μm) and 1/16 in., respectively.

Polymer samples were collected "in-situ" on a $^1/_{16}$ in. o.d. × $^3/_4$ in. long section of stainless steel tubing. The tubing was attached to a small rectangular glass slide (1 in. by $^1/_4$ in.). The glass slide was placed diagonally into the cell approximately 5−7 cm. below the tip of the atomizer. The sample stage was held in place using finely meshed steel foil. To prevent the vent valve from plugging, a $^1/_4$ in. diameter 0.5 μm frit filter was placed after the Swagelok O-seal straight thread male connector located at the bottom of the precipitator.

Procedure. The stabilizer/CO_2 solution was agitated in the variable volume cell at ∼200 bar for >2 h to achieve complete dissolution. Before the PCA experiment, pure CO_2 was pumped through the sapphire precipitator to set the pressure and flow rate at 35 mL/min. During this time, the manual syringe pump valve F was closed and valve A was opened to bring the CO_2/stabilizer solution to the experimental pressure. Next, the stabilizer/CO_2 solution was delivered to the sapphire precipitator by simultaneously opening valve C and closing valve B. After 25 s of flowing of this solution at 35 mL/min (∼1 residence volume), the automated syringe pump was switched from the constant pressure (predetermined ΔP for 1.0 mL/min) to the constant flow mode (set at 1.0 mL/min). This procedure minimized the time required for the automated syringe pump to achieve the desired constant flow rate of the polymer solution. By opening valve D, the polymer solution was sprayed for 25 s at 1.0 mL/min into the continuous phase (CO_2 with stabilizer) flowing at 35 mL/min. The solution spray was stopped by closing valve D. Next, valve B was opened to pump pure CO_2 through the vessel for 10 min at the same CO_2 flow rate to remove any residual organic solvent. After drying, the CO_2 was depressurized for ∼20 min at the operating temperature.

Table 1. Properties of Polymeric Stabilizers Used in This Study

stabilizer	M_w (g/mol)	concn (wt %)	temp (°C)	cloud point (bar)
poly(FOA)	1.0×10^6	1.0	24	110
			45	187
		0.70	45	182
	1.0×10^4	0.73	45	162
PS-*b*-PFOA	3.7K/27.5K	0.93	45	176
		0.01	25	96.5

Results

The phase behavior of the stabilizer/CO_2 system must be known in order to prepare homogeneous solutions. Cloud point data for the stabilizers used in this study are given in Table 1. At 25 °C, 1.0 wt % poly(FOA) (1.0×10^6 g/mol) phase separates at 110 bar. This result agrees with the behavior of detailed poly(FOA) cloud point curves for temperature between 30 and 80 °C and solute concentrations from 0.09−4.84 wt %, respectively.[30] For poly(FOA) homopolymer, lower critical solution temperature (LCST) phase behavior is observed with a critical concentration estimated between 1.0 and 2.0 wt % for all pressures investigated. For a 0.93 wt % solution of 3.7K/27.5K PS-*b*-poly(FOA) in CO_2, the cloud point is 176 bar. Here the insolubility of the 3.7K PS block in CO_2 raises the cloud point pressure of the block copolymer far above that of poly(FOA).

PMMA Stabilized by Poly(FOA). A summary of the experimental results is presented in Table 2. All of the morphologies were reproduced at least once at each condition. When PMMA is sprayed into CO_2 without stabilizer using the standard nozzle, a highly flocculated morphology is formed, as shown in Figure 2. The size of the flocculated primary particles created by jet atomization and drying range from 0.1 to 1.0 μm. During the spray process, several visual observations were recorded. A cloud of PMMA precipitate was observed to accumulate below the tip of the capillary atomizer approximately 5 s into the spray. After ~15 s, accumulation of the PMMA on the inside wall of the precipitator was observed. Fluctuations in refractive index due to concentration inhomogeneities were observed visually ~5 s into the spray, indicating incomplete mixing of the suspended solvent droplets and CO_2. These striations were observed in all of the experiments with the standard nozzle. Similar observations have been described in detail elsewhere.[12]

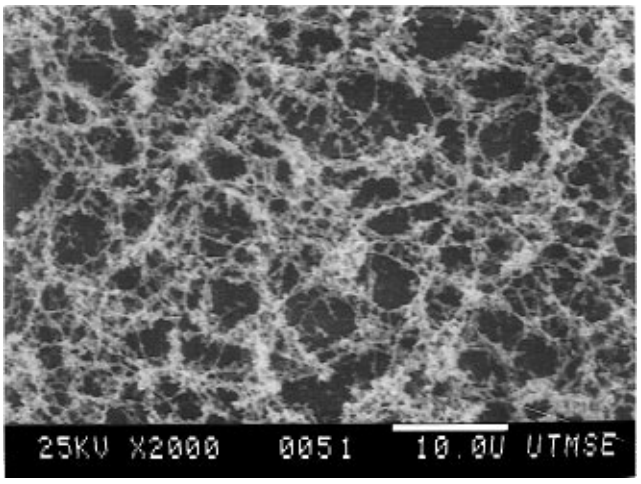

Figure 2. SEM micrograph of PMMA precipitated by spraying a 1.0 wt % PMMA/MEK solution through 50 μm standard capillary nozzle into CO_2 at a temperature and pressure of 23 °C and 124.1 bar.

The results of addition of 0.01 wt % poly(FOA) (0.76 g/g of PMMA) to the flowing CO_2 to stabilize PMMA microparticles precipitated from a 1.0 wt % PMMA/MEK solution are shown in Figure 3. As is clearly apparent, far less flocculation is observed with the addition of poly(FOA). Furthermore, many individual PMMA primary particles are present which range in size from 0.1 to 0.5 μm. During precipitation, a cloud of PMMA particles was observed to accumulate throughout the precipitator below the tip of the capillary nozzle within 10 s; however, no PMMA was detected on the inside wall of the precipitator.

With a higher concentration of poly(FOA), 0.05 wt % (3.73 g/g of PMMA), the size of the flocculated groups is reduced to 1−4 μm, as shown in Figure 4. Furthermore, the fraction of individual nonflocculated 0.1−0.5 μm primary particles is considerably larger. The entire view cell below the tip of the atomizer was observed to turn slightly opaque after 10 s of spraying. Upon further increasing the poly(FOA) concentration to 1.0 wt % (104 g/g PMMA), a different result was observed. The vessel did not turn opaque during precipitation. Furthermore, no PMMA precipitate was collected on either the 0.5 μm frit filter or the glass sample stage.

With the use of the coaxial nozzle, the size of the flocculated groups is reduced to 1−2 μm for a 0.01 wt

Table 2. Stabilizer Concentration, Visual Observations, and Morphology of 1.0 wt % PMMA in MEK and PS in Toluene Solutions Sprayed through a Coaxial Nozzle into CO_2 at 23 °C and 124.1 bars Loaded with Poly(FOA)-Based Stabilizers

stabilizer	concn (wt %)	polymer	visual: flocc/accum[h]	primary particles (μm)	microparticle structure
none	0.0	PMMA	no/yes[a]	0.1−0.5	flocculated
	0.0	PMMA	yes/yes	0.1−0.5	flocc groups > 50 μm
	0.0	PS	yes/yes	0.1−0.5	flocc groups > 50 μm
poly(FOA)	0.01	PMMA	no/no[a]	0.1−0.5	partially flocc
	0.01	PMMA	no/no	0.1−0.5	slightly flocc, 1−2 μm
	0.05	PMMA	no/no[a]	0.1−0.5	slightly flocc, 1−4 μm
	1.0	PMMA	no/no	<0.1[d]	precipitate
	0.05[b]	PS	yes/slight	0.1−0.5	partially flocc, 10−50 μm
	0.05[c]	PS	yes/yes	0.1−0.5	partially flocc, 10−50 μm
PS-*b*-PFOA[e]	0.00009	PS	yes/yes	0.1−0.5	flocculated
	0.0014	PS	yes/yes	0.1−0.5	flocculated
	0.0055	PS	yes/yes	0.1−0.5	partially flocc, 10−50 μm
	0.0076	PS	no/slight	0.1−0.5	no flocc, 10-−50 μm
	0.01	PS	no/no	0.1−0.3	no flocc
	0.05	PS	no/no	0.1−0.3	no flocc
Poly(FOA)/ PS-*b*-PFOA[e]	0.0104[f]	PS	no/no	0.1−0.5	partially flocc, <10 μm
	0.011[g]	PS	yes/yes	0.1−0.5	partially flocc, 10−20 μm

[a] Standard nozzle. [b] 1.0×10^4 g/mol. [c] 1000k M_w. [d] Estimated. [e] $P = 137.9$ bars. [f] 75/25 PS-*b*-PFOA/PFOA mixture. [g] 60/40 PS-*b*-PFOA/PFOA mixture. [h] Visual accumulation of precipitate on inside wall of the sapphire vessel.

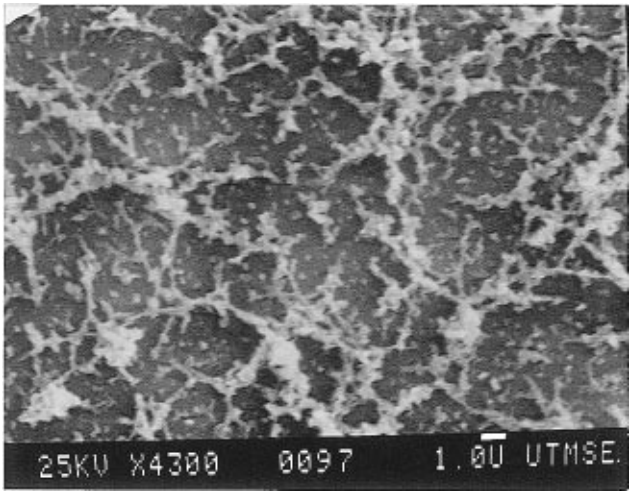

Figure 3. SEM micrograph of PMMA precipitated by spraying a 1.0 wt % PMMA/MEK solution through a 50 μm standard capillary nozzle into a 0.01 wt % PFOA/CO_2 solution at a temperature and pressure of 23 °C and 124.1 bar.

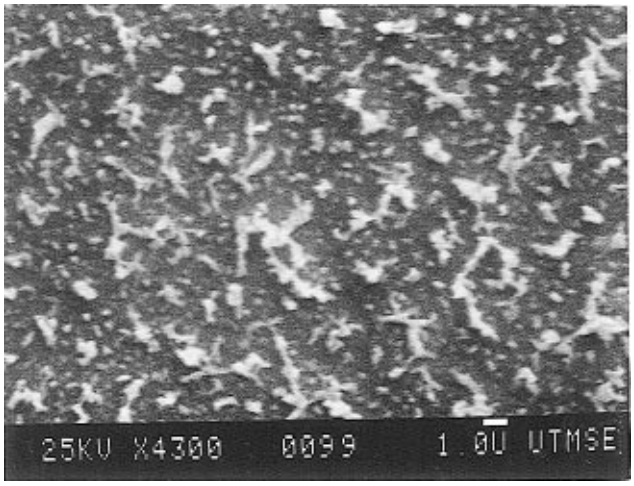

Figure 4. SEM micrograph of PMMA precipitated by spraying a 1.0 wt % PMMA/MEK solution through a 50 μm standard capillary nozzle into a 0.05 wt % PFOA/CO_2 solution at a temperature and pressure of 23 °C and 124.1 bar.

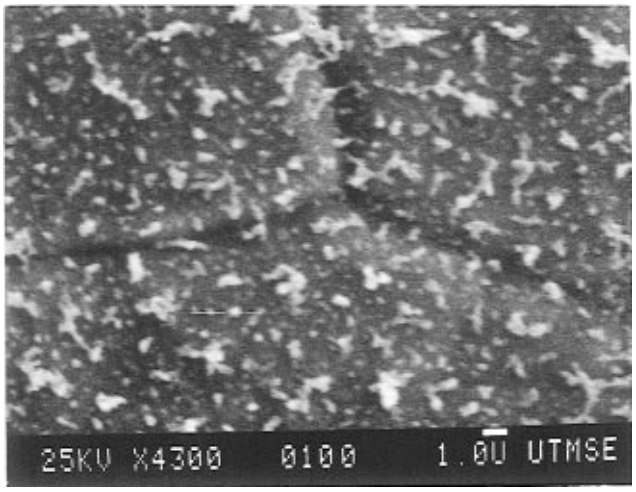

Figure 5. SEM micrograph of PMMA precipitated by spraying a 1.0 wt % PMMA/MEK solution through a 50 μm coaxial capillary nozzle into a 0.01 wt % PFOA/CO_2 solution at a temperature and pressure of 23 °C and 124.1 bar.

% poly(FOA) solution (0.76 g of poly(FOA)/g of PMMA), as shown in Figure 5. The fraction of nonflocculated 0.1−0.5 μm primary particles is considerably larger than that observed with the standard nozzle (Figure 3).

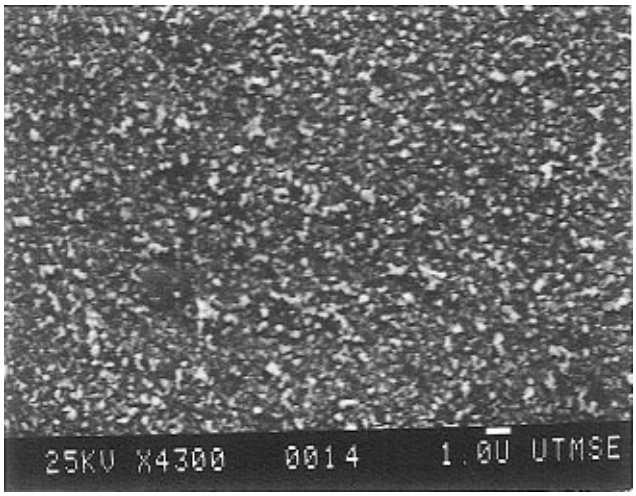

Figure 6. SEM micrograph of PS precipitated by spraying a 1.0 wt % PS/toluene solution through a 50 μm coaxial capillary nozzle into a 0.01 wt % PS-*b*-PFOA/CO_2 solution at a temperature and pressure of 23 °C and 137.9 bar.

Although the stabilizer concentration is only 0.01 wt %, these microparticles resemble those formed in the standard nozzle with a higher poly(FOA) concentration of 0.05 wt % (Figure 4). During precipitation, the entire cell turned opaque within 10 s.

For both types of nozzles with stabilizer, particles did not accumulate on the walls of the sapphire vessel. Recently, we found that particle sizes of PMMA measured by *in-situ* turbidimetry for other stabilizers agreed with those determined by SEM, after depressurization.[45] This consistency supports the particle sampling methodology. Therefore, the samples obtained on the $^1/_{16}$ in. stainless steel tube are likely to be representative of the particles produced throughout the precipitator.

PS Stabilized by PS-*b*-poly(FOA). All of the PS solutions were atomized into CO_2 through the coaxial nozzle. For these experiments, the CO_2 pressure was increased from 124.1 to 137.9 bar to fully dissolve the stabilizer. When a 1.0 wt % PS/toluene solution was sprayed into pure CO_2, a fine suspension of PS precipitate was observed throughout the precipitator. After ∼10 s, individual particles were observed within the dense suspension, indicating that extensive flocculation had occurred. PS flocculation was accompanied by accumulation of product on the inside wall of the sapphire vessel. Because of the extensive accumulation, less PS collected on the sample stage; however, the morphology remained highly flocculated. As shown in Table 2, the diameters of the large floccs were well in excess of 50 μm. While a few larger microparticles were observed, the majority of the primary particles ranged from 0.1 to 1.0 μm in diameter.

The results for a 0.01 wt % PS-*b*-poly(FOA) (0.76 g/g of PS) solution are shown in Figure 6. Compared to the PS particles with no stabilizer (Figure 2) and the PMMA stabilized with 0.01 wt % poly(FOA) homopolymer (Figure 5), dramatic changes are apparent. Here individual, non-flocculated PS primary particles are formed which range in size from 0.1 to 0.3 μm. Throughout the spray, flocculation and accumulation were clearly absent in the fine PS suspension.

When the PS-*b*-poly(FOA) concentration was lowered to 0.0076 wt % (0.57 g/g PS), an increase in microparticle flocculation was observed, as shown in Figure 7A. During precipitation, this flocculation was not apparent by visual observation. However, as the PS-*b*-poly(FOA) concentrations were lowered even further (Table 1), PS

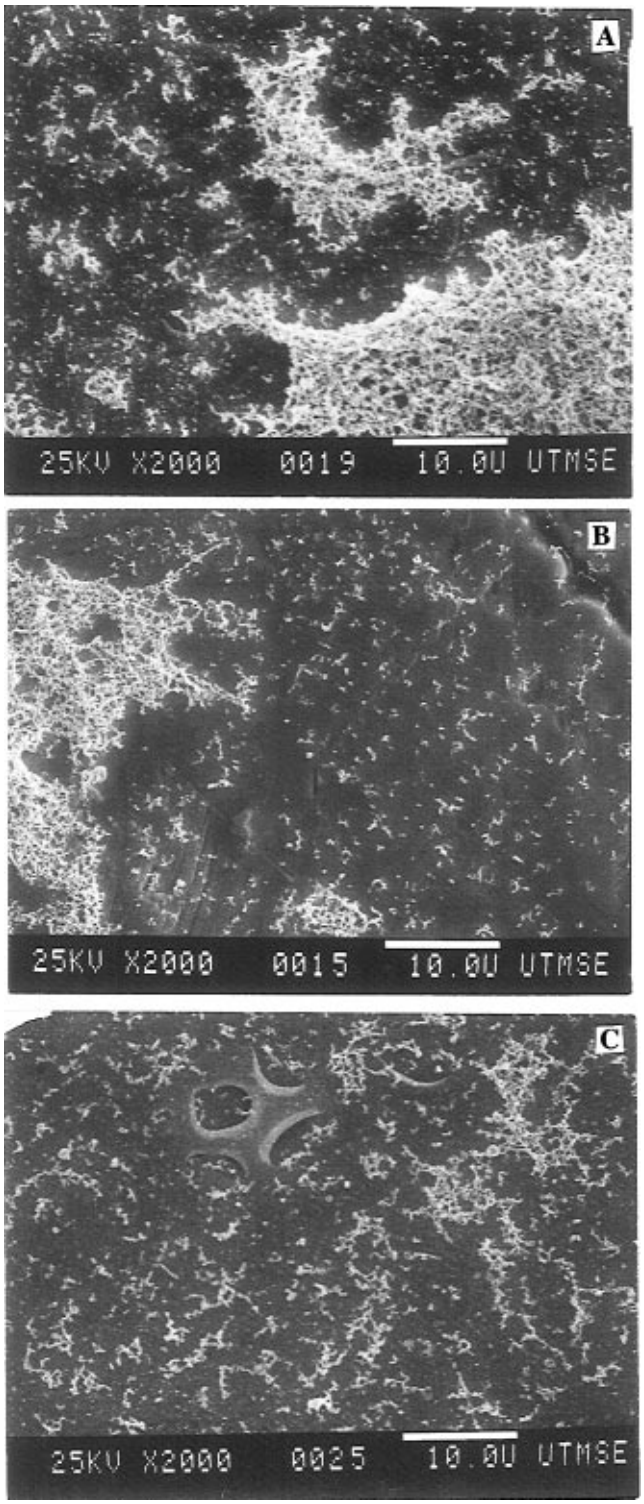

Figure 7. SEM micrographs of PS precipitated by spraying a 1.0 wt % PS/toluene solution through a 50 μm coaxial capillary nozzle into (A) 0.0076 wt % PS-*b*-PFOA/CO_2 solution, (B) 0.5 wt % PFOA (1.0×10^4 g/mol), and (C) 0.0078 wt % PS-*b*-PFOA and 0.0026 wt % PFOA (0.011 wt % total) at a temperature and pressure of 23 °C and 137.9 bar.

flocculation became visible in the precipitator. As shown in Figure 7B, severe PS flocculation occurred with the use of 0.05 wt % poly(FOA) homopolymer (1.0×10^4 g/mol) as a stabilizer. Increasing the M_w to 1.0×10^6 g/mol did not prevent flocculation; it merely delayed the onset of flocculation, as observed during the experiment.

In an attempt to achieve PS stabilization with a smaller amount of block copolymer, PS-*b*-poly(FOA) was mixed with the homopolymer, poly(FOA). The composition of the resulting solution was 0.0026 wt % poly(FOA) (M_w=1.0×10^6 g/mol) and 0.0076 wt % PS-*b*-poly(FOA), corresponding to a total stabilizer concentration of 0.0104 wt % (75/25 PS-*b*-poly(FOA)/poly(FOA)). As shown in Figure 7C, individual submicron particles are produced along with flocculated domains <10 μm in size. During precipitation, no flocculation or accumulation was observed, unlike the case for the same concentration of PS-*b*-poly(FOA) without poly(FOA). Flocculation was observed visually when the PS-*b*-poly(FOA)/poly(FOA) ratio was lowered to 60/40 for the same overall stabilizer concentration (Table 2).

Discussion

PCA Fundamentals. Before describing the role of the stabilizer, we provide a brief summary of the microparticle formation mechanism. The key features are jet breakup, the mass transfer pathway through the phase diagram, the collisions and drying of the suspended droplets, and the plasticization of the polymer by CO_2 (and residual solvent). The jet breakup mechanism is a function of the dimensionless Weber number (N_{We}).[46,47] N_{We} is the ratio of the inertial forces to surface tension forces and is given by $N_{We} = \rho_A v^2 D/\gamma$, where ρ_A is the antisolvent density, v is the velocity of the jet relative to that of the CO_2, D is the jet diameter, and γ is the interfacial tension. Because of the high solution velocity, i.e., ~849 cm/s at a flow rate of 1.0 mL/min, combined with a small interfacial tension and high CO_2 density, the jet break up mechanism is dominated by intense atomization rather than Raleigh instabilities.[13,16] Thus, the process has the potential to form very small particles if they do not agglomerate.

A ternary phase diagram with accompanying mass transfer pathways may be used to describe the PCA phase separation mechanism.[8,12,13,16] When the mass transfer pathway crosses the binodal curve into the metastable region, phase separation occurs by nucleation and growth. After crossing the spinodal region into the metastable region, the remaining phase separation takes place by spinodal decomposition into the unstable region. Because the 1.0 wt % solutions used in this study follow a mass transfer pathway that crosses the binodal curve below the plait point (critical point), polymer-rich domains nucleate and grow within a solvent continuous phase.[8,12,13,16] Polymer vitrification occurs when the mass transfer pathway crosses into the glassy region of the phase diagram. However, due to plasticization by CO_2, the PMMA microparticles do not vitrify until the solution is depressurized at the end of the experiment.

Recently, considerable insight has been shed into the phase separation and flocculation mechanisms in PCA.[12] Two parts of the mass transfer pathway may be considered separately: atomization and jet break up followed by recirculation and suspension of the particles throughout the entire precipitation vessel. The standard nozzle provides intense atomization but poor mixing of the suspended particles that leave the jet due to the low CO_2 velocity. The poor mixing is observed in the form of refractive index gradients throughout the precipitator. With the coaxial nozzle, atomization in the jet is less prevalent due to the smaller relative velocity between the solution phase and continuous phase. However, recirculation and mixing of the suspended droplets is much more intense due to the high CO_2 velocity. With the standard nozzle, atomization plays a more prevalent role in the phase separation mechanism than for the coaxial nozzle. Since the jet velocity

is typically 1000 cm/s, the characteristic time for precipitation in the first 0.1 cm of the jet is 10^{-4} s. Outside of the jet, the characteristic time for stabilization of the suspensions throughout the precipitator is on the order of seconds.

The mixing of the liquid solvent and CO_2 is endothermic since the solvent expands. In this study, the temperature was 23 °C and the CO_2 density was 0.86 g/mL. At this high density, the expansion of liquid solvent is small producing a small temperature decrease. Upon cooling, the stabilizer remains soluble.

When polymers are plasticized by CO_2, particle−particle and/or particle−wall collisions cause primary particles to flocculate and agglomerate. Particles may also flocculate as they fall onto the sample stage located below the atomization nozzle. When two plasticized particles collide, they initially flocculate at the point of contact. If they contain a sufficient amount of solvent, minimization of the particle surface area by coalescence can create larger, more agglomerated structures.

Mechanism for Stabilized PCA. In PCA with the standard nozzle, it was observed visually that a significant amount of precipitate is formed within the jet. This observation was unmistakable. If no stabilization took place inside the jet, the PMMA particles would have been much more flocculated than those shown in Figure 3 or 4. Thus, the stabilizers become active in time frames on the order of the residence time in the jet, which is less than 1 ms. The diffusion length of the surfactant may be estimated by the relationship $L = (Dt)^{1/2}$. Diffusion coefficients are higher in supercritical fluids than in liquids, and often reach 10^{-4} cm^2/s. For a time of 10^{-4} s, $L = 1\ \mu$m. Because the surfactant was present throughout the continuous phase, it may be expected that it could begin to adsorb to 0.1 μm particles in 10^{-4} s. However, the majority of the stabilization likely took place outside of the jet. Smaller, less-flocculated particles were formed with the coaxial nozzle, where a greater fraction of the mass transfer takes place outside of the jet, providing more time for diffusion and adsorption of stabilizer, up to seconds. In contrast, the time frame for stabilization in dispersion polymerization is typically minutes to hours.

For a poly(FOA) concentration of 0.05 wt % (Figure 4), the coverage of the PMMA primary particles was sufficient to almost completely suppress flocculation and agglomeration. However, when the poly(FOA) in CO_2 concentration was increased further to 1.0 wt % (104 g of poly(FOA)/g of PMMA), the solution did not turn opaque and no PMMA precipitate was collected. These observations suggest that the excessive amount of poly(FOA) may act as a cosolvent for PMMA, keeping it in solution.

Compared to the PMMA particles stabilized with 0.051 wt % poly(FOA) (Figure 5), far more uniform, less flocculated 0.1−0.3 μm PS microparticles were produced with only 0.01 wt % PS-*b*-poly(FOA) (Figure 6). The performance of each of these poly(FOA)-based stabilizers may be expected to be related directly to its activity at the polymer−CO_2 interface. The adsorption dynamics and equilibrium of the stabilizers at the polymer−CO_2 interface are key properties for understanding the rapid latex stabilization during PCA. The adsorption equilibrium or interfacial activity of a stabilizer may be obtained from the decrease in the interfacial tension, γ, between the dispersed phase and CO_2 as a function of the stabilizer concentration. Recently, a novel tandem variable-volume pendant drop tensiometer has been used to measure the effect of poly(FOA) on γ for the poly(ethylhexyl acrylate) (PEHA)−CO_2 interface[32] and of PS-*b*-poly(FOA) for the PS oligomer−CO_2 interface.[48] With the addition of poly(FOA) to the PEHA−CO_2 system, γ actually increases. This is due to depletion of poly(FOA) at the interface relative to the bulk CO_2. The weak poly(FOA) absorption may be attributed to a small number of adsorbed segments and a large number of segments in loops and tails. Despite the small degree of adsorption, the long loops and tails can still provide steric stabilization of latexes in dispersion polymerization and in this study.

With the addition of PS-b-poly(FOA) to the PS−CO_2 system, a break in γ is observed at ∼0.001 wt % which likely indicates a critical micelle concentration (cmc). Above the cmc, this stabilizer lowers γ between PS and CO_2 from 2.2 to 1.2 dynes/cm.[48] It adsorbs much more strongly in the interfacial region than poly(FOA), which must be due to the PS anchor block. This stronger adsorption is consistent with the more uniform PS latex particles in Table 2 for PS-*b*-poly(FOA) verses poly(FOA).

For the experiments containing mixtures of both stabilizers, poly(FOA) homopolymer did not enhance stabilization relative to PS-*b*-poly(FOA). In the PCA time frames, these results suggest that the more strongly adsorbing PS-*b*-poly(FOA) dominates the stabilization mechanism, and that the poly(FOA) homopolymer does not tend to adsorb significantly to the poly(FOA) tails of PS-*b*-poly(FOA).

For the poly(FOA) stabilizer in the flowing CO_2 phase, it was unknown what fraction of the stabilizer adsorbs to the polymer. During a 25 s spray at a constant solution flow rate of 1.0 mL/min, 3.7 mg of PMMA were sprayed. For a poly(FOA) concentration of 0.01 wt % (based upon CO_2), ∼756 mg of poly(FOA)/g of PMMA were present at the end of the spray. In contrast, the amount of poly(FOA) ranged from 2.5−160.0 mg/g of MMA, in a typical dispersion polymerization. Because of the small polymer concentration in PCA, the PMMA-rich domains are only exposed to a small fraction of the total amount of the poly(FOA) present throughout the precipitator. The unattached poly(FOA) is removed by the continuously flowing CO_2.

In the dispersion polymerization of PMMA with poly(FOA), chemical grafting of the stabilizer can be present.[30] In the PCA process, grafting is not present, yet the extremely rapid stabilization of the particles is sufficient to minimize flocculation.

There are some differences in the particles produced by dispersion polymerization and PCA with stabilizers. The primary particles in Figure 5 and especially in Figure 6 are much less than 1.0 μm in diameter, compared with somewhat larger particles of 2.1−2.9 μm produced by dispersion polymerization using 0.24−4.5 wt % poly(FOA) stabilizer. Smaller 1.0 μm microspheres were produced by polymerization with 16.0 wt % poly(FOA); however, 1.55 μm microspheres were also present in a bimodal size distribution.[30] After 4 h of MMA polymerization using 4.5 wt % poly(FOA) (based on MMA), 92% mass conversion was obtained. This corresponds to an approximate PMMA concentration in CO_2 of 20 wt %, whereas it was only 0.03 wt % in PCA. Also, the stabilizer to polymer weight ratio was 1.0 (PS-*b*-poly(FOA)/PS) to 5.0 (poly(FOA)/PMMA) in the PCA process, whereas it was typically 0.005−0.17 in the polymerization of PMMA with poly(FOA).

Conclusions

Steric stabilizers can be used in the PCA process to produce uniform microparticles of amorphous polymers,

even when they are plasticized by CO_2. Fluoro acrylate-based stabilizers including poly(FOA) and PS-*b*-poly(FOA) can be introduced via the CO_2 phase, as they are soluble. Without stabilizer, PMMA and PS are highly flocculated due to plasticization by CO_2. With a poly(FOA) homopolymer concentration of 0.05 wt %, flocculation of PMMA is almost completely removed.

Using the coaxial nozzle, highly uniform 0.1−0.3 μm PS microparticles are formed with minimal flocculation with the addition of only 0.01 wt % PS-*b*-poly(FOA). By delaying precipitation with the coaxial nozzle, the stabilizers become even more effective at preventing flocculation. PS-*b*-poly(FOA) stabilizes the latex better than poly(FOA), since it adsorbs more strongly to the interface. The combination of extremely rapid phase separation in PCA, which is much faster than for conventional liquid antisolvents, along with the steric stabilization, account for the submicron particles. The prevention of flocculation in the jet, where precipitation was observed visually, required the stabilizer to become active in 10^{-4} s. In the suspension, steric stabilization continues for seconds throughout the precipitator.

Three key benefits of the use of a stabilizer in the PCA process have been illustrated: (1) demonstration of the ability to form uniform nonflocculated submicron particles; (2) a clearer understanding of the mechanism of PCA, since the complication of flocculation was removed; and (3) a new means to study stabilization of latexes of submicron particles in CO_2.

Acknowledgment. At UT, we are grateful for support from NSF(CTS-9218769), the Texas Advanced Technology Program (3658-198), and the Separation Research Program at the University of Texas. In addition, we thank ISCO Corp. for the donation of the high pressure syringe pump. We also thank Tim Young for his assistance with the PCA experiments. At UNC, we are grateful to the NSF (Presidential Faculty Fellowship, J.M.D.) and the Consortium for the Synthesis and Processing of Polymeric Materials in CO_2 sponsored by Air Products and Chemicals, Bayer, BF Goodrich, DuPont, Eastman Chemical, GE, Hoechst-Celanese, and Xerox.

References and Notes

(1) Dixon, D. J., Ph.D. Thesis, The University of Texas at Austin, 1992.
(2) Matson, D. W.; Peterson, R. C.; Smith, R. D. *J. Mater. Sci.* **1987**, *22*, 1919−1928.
(3) Peterson, R. C.; Matson, D. W.; Smith, R. D. *Polym. Eng. Sci.* **1987**, *27*, 1693−1697.
(4) Lele, A. K.; Shine, A. D. *AICHE J.* **1992**, *38*, 742−752.
(5) Boen, S. N.; Bruch, M. D.; Lele, A. K.; Shine, A. D. In *Polymer Solutions, Blends and Interfaces*; Noda, I.; Rubingh, D. N., Ed.; Elsevier Science Publishers: New York, 1992; pp 151-172.
(6) Lele, A. K.; Shine, A. D. *Ind. Eng. Chem. Res.* **1994**, *33*, 1476−1485.
(7) Tom, J. W.; Debenedetti, P. G.; Jerome, R. *J. Supercrit. Fluids* **1994**, *7*, 9−29.
(8) Mawson, S.; Johnston, K. P.; Combes, J. R.; DeSimone, J. M. *Macromolecules* **1995**, *28*, 3182−3191.
(9) Dixon, D. J.; Bodmeier, R. A.; Johnston, K. P. *AIChE J.* **1993**, *39*, 127−139.
(10) Randolph, T. W.; Randolph, A. D.; Mebes, M.; Yeung, S. *Biotechnol. Prog.* **1993**, *9*, 429−435.
(11) Yeo, S.; Lim, G.; Debenedetti, P. G.; Bernstein, H. *Biotechnol. Bioeng.* **1993**, *41*, 341−346.
(12) Mawson, S.; Kanakia, S.; Johnston, K. P. *J. Appl. Polym. Sci.* In press **1996**.
(13) Dixon, D. J.; Johnston, K. P. *J. Appl. Polym. Sci.* **1993**, *50*, 1929−1942.
(14) Yeo, S.-D.; Debenedetti, P. G.; Radosz, M.; Schmidt, H.-W. *Macromolecules* **1993**, *26*, 6207−6210.
(15) Yeo, S.-D.; Debenedetti, P. G.; Radosz, M.; Giesa, R.; Schmidt, H.-W. *Macromolecules* **1995**, *28*, 1316−1317.
(16) Luna-Bàrcenas, G.; Kanakia, S. K.; Sanchez, I. C.; Johnston, K. P. *Polymer* **1995**, *36*, 3173−3182.
(17) Dixon, D. J.; Luna-bàrcenas, G.; Johnston, K. P. *Polymer* **1994**, *35*, 3997−4006.
(18) Bodmeier, R.; Wang, H.; Dixon, D. J.; Mawson, S.; Johnston, K. P. *Pharm. Res.* **1995**, *12*, 1211−1217.
(19) Falk, R.; Randolph, T.; Meyer, J. D.; Kelly, R. M.; Manning, M. C. *J. Controlled Release.* In press. **1996**.
(20) Mawson, S.; Kanakia, S.; Johnston, K. P. *Polymer*. In press. **1996**.
(21) Wang, H., M.S. Thesis, The University of Texas at Austin, 1993.
(22) Chow, T. S. *Macromolecules* **1980**, *13*, 362−364.
(23) Condo, P. D.; Sanchez, I. C.; Panayiotou, C. G.; Johnston, K. P. *Macromolecules* **1992**, *25*, 6119−6127.
(24) Kalopsiros, N. S.; Paulaitis, M. E. *Chem. Eng. Sci.* **1993**, *48*, 23−40.
(25) Wissinger, R. G.; Paulaitis, M. E. *J. Polym. Sci., Part B, Polym. Phys.* **1991**, *29*, 631−633.
(26) Condo, P. D.; Johnston, K. P. *J. Polym. Sci.: Part B, Polym. Phys.* **1992**, *32*, 523−533.
(27) Condo, P. D.; Paul, D. R.; Johnston, K. P. *Macromolecules* **1994**, *27*, 365−371.
(28) O'Neill, M. L., Ph.D. Thesis, Carleton University, 1994.
(29) DeSimone, J. M.; Maury, E. E.; Menceloglu, Y. Z.; McClain, J. B.; Romack, T. J.; Combes, J. R. *Science* **1994**, *265*, 356−359.
(30) Hsiao, Y.-L.; Maury, E. E.; DeSimone, J. M.; Mawson, S.; Johnston, K. P. *Macromolecules* **1995**, *28*, 8159−8166.
(31) Canelas, D. A.; Betts, D. E.; DeSimone, J. M. *Macromolecules*, **1996**, *29*, 2818−2821.
(32) O'Neill, M. L.; Yates, M. Z.; Harrison, K. L.; Johnston, K. P.; Canelas, D. A.; Betts, D. E.; DeSimone, J. M.; Wilkinson, S. P. *Macromolecules.* Submitted. **1996**.
(33) Peck, D. G.; Johnston, K. P. *Macromolecules* **1993**, *26*, 1537−1545.
(34) Hoefling, T. A.; Enick, R. M.; Beckman, E. J. *J. Phys. Chem.* **1991**, *95*, 7127−7129.
(35) Hoefling, T.; Stofesky, D.; Reid, M.; Beckman, E. J.; Enick, R. M. *J. Supercrit. Fluids* **1992**, *5*, 257−241.
(36) DeSimone, J. M.; Guan, Z.; Elsbernd, C. S. *Science* **1992**, *257*, 945−947.
(37) Newman, D. A.; Hoefling, T. A.; Beitle, R. R.; Beckman, E. J.; Enick, R. M. *J. Supercrit. Fluids* **1993**, *6*, 205−210.
(38) Hoefling, T. A.; Newman, D. A.; Enick, R. M.; Beckman, E. J. *J. Supercrit. Fluids* **1993**, *6*, 165−171.
(39) Kissa, E. *Fluorinated Surfactants Synthesis, Properties, Applications*; Marcel Dekker, Inc: New York, 1994; Vol 50.
(40) Harrison, K. L.; Goveas, J.; Johnston, K. P.; O'Rear, III, E. A. *Langmuir* **1994**, *10*, 3536−3541.
(41) McHugh, M. A.; Krukonis, V. J. *Supercritical Fluid Extraction Principles and Practice*, 2nd ed.; Butterworths: Stoneham, MA, 1994.
(42) Johnston, K. P.; Harrison, K.; Clarke, M. J.; Howdle, S. M.; Heitz, M. P.; Bright, F. V.; Carlier, C.; Randolph, T. W. *Science* **1995**, *271*, 624−626.
(43) McClain, J. B.; Londono, D.; Combes, J. R.; Romack, T.; Canelas, D. A.; Betts, D. E.; Wignall, G. D.; Samulski, E. T.; DeSimone, J. M. *J. Am. Chem. Soc.* **1996**, *118*, 917−918.
(44) Guan, Z.; DeSimone, J. M. *Macromolecules* **1994**, *27*, 5527−5532.
(45) Mawson, S.; Yates, M. Z.; O'Neill, M. L.; Johnston, K. P. *Langmuir.* Submitted. **1996**.
(46) Lefebvre, A. H. *Atomization and Sprays*; Hemisphere Publishing Corporation: New York, 1989.
(47) Bayvel, L.; Orzechowski, Z. *Liquid Atomization*; Taylor and Francis: Washington, DC, 1993.
(48) Harrison, K. L.; Johnston, K. P. Unpublished results.

MA961048T